

Initial Assessment of Hydrocarbon Potential in the Alor Basin Using Integrated Hydrographic Data

Irena Hana Hariyanto* and Alvina Viasty

Department of Geomatics Engineering, Institut Teknologi Sepuluh Nopember, Surabaya, 60111, Indonesia

Abstract. Identification of hydrocarbons is a preliminary step in oil and gas exploration. By using hydro-acoustic data, this study aims to assess the hydrocarbon potential of the Alor Basin. Several data were acquired during the Jala Citra III Expedition in the Flores Sea in 2023, including Multibeam Echosounder and Marine Magnetometer. Bathymetric processing indicates that the Alor Basin reaches a maximum depth of 4,777.68 meters. The seabed is predominantly composed of clay-rich sediments, inferred to result from the deposition of fine-grained marine biogenic material or volcanic ash. This sediment analysis indicates depositional environments that may influence hydrocarbon generation and accumulation processes. Marine magnetometer data revealed residual magnetic anomalies ranging from $-1,031.022$ nT to 361.214 nT, with negative anomalies corresponding to intense tectonic activity. This interpretation is supported by fault structures analysis along the seismic profiles from the Marine Geological Research and Development Centre (P3GL), which may act as structural traps or migration pathways for hydrocarbons. Integrated bathymetric, magnetic, and seismic interpretations explain the basin's geodynamic evolution and its correlation to hydrocarbon system formation. The fault patterns, seabed morphology, and magnetic anomalies all indicate active tectonic processes, suggesting that the Alor Basin holds significant potential for hydrocarbon accumulation and future exploration.

1 INTRODUCTION

Ocean basins are crucial for storing natural resources, including oil and gas. Currently, there are 128 oil and gas basins in Indonesia, and approximately 53% of these remain unexplored [1]. These basins typically form in areas of interplate subduction that result in volcanic activity. This creates back-arc basins and fore-arc basins along volcanic belts. Back-arc basins are underwater basins formed behind island arcs and can produce large quantities of crude oil decades later [2].

Research in Eastern Indonesian waters has revealed significant geological structures, revealing the existence of seven basins in the Flores Sea and its surroundings. One of the identified basins is the Alor Basin in the eastern Flores Sea. The Alor Basin is located in the back-arc region of the Lesser Sunda Islands (LSI) and contains submarine volcanoes. This leads to the formation of back-arc thrust faults, which at certain points can lead to plate collisions, leading to deformation and the formation of strong thrust faults. This situation is closely related to sedimentation, which can store hydrocarbons used in oil and gas exploration [3].

Petroleum, or hydrocarbons, is a general term for organic compounds found in crude oil and natural gas [4]. Hydrocarbons in the ocean are formed from the accumulation of organic matter, such as plankton and marine plants, trapped by seafloor sediments over millions of years. In geophysics, these traps are referred to as reservoir rocks. Hydrocarbon identification is generally performed through seismic analysis to determine the geological structure and reservoir potential before drilling [5]. This study used a combination of hydrographic survey data and seismic sections to identify the presence of hydrocarbons in the Alor Basin.

This study utilizes various hydrographic instruments for further processing and analysis of the potential presence of hydrocarbons in the Alor Basin. Sounding data from a multibeam echosounder can show water depth and backscatter data can determine the characteristics of sediment in the first layer or seabed [6]. Magnetometer data is used to identify magnetic anomalies in the study area [7]. Areas suspected of containing hydrocarbons will have different magnetic

* Corresponding author: irena@its.ac.id

values from their surroundings. Hydrographic surveys are conducted as an innovation and support in the hydrocarbon identification process. This is in line with Sustainable Development Goals point nine regarding industry, innovation, and infrastructure.

2 METHOD

2.1 Research Location

This research location is in the eastern Flores Sea, specifically in the Alor Basin. Figure 1 shows the eastern Flores Sea, Indonesia. The area is located between 7°01'51" to 8°23'56" South and 122°54'35" to 124°40'55" East. This water is classified as tropical water and is famous for its rich marine natural resources.

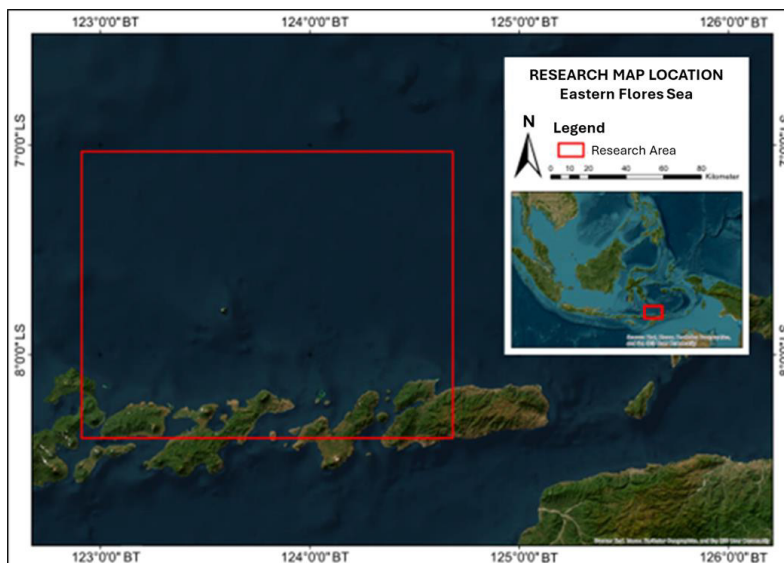


Fig. 1. Research Location in the East Flores Sea, Alor Waters

2.2 Data and Equipment

The data used in this study comes from the Jala Citra III Expedition, acquired from March to May 2023. The data was installed on the KRI SPICA 934, owned by the Indonesian Navy's Center for Hydro-Oceanography (Pushidrosal), which was used during the expedition. The details of the data utilized in this research are described in the table below.

Table 1. Setting Word's margins.

No	Data	Information
1	Raw Bathymetry and Backscatter Strength	Kongsberg EM 302 Multibeam Echosounder
2	Tides	TPXO 8.0 model
3	Sound Velocity	Sound Velocity Profiler (SVP)
4	Magnetic Value	G-882 Cesium Marine Magnetometer

In addition, this study also used declination, inclination, and IGRF correction data from the National Geophysical Data Center (NGDC) website of the National Oceanic and Atmospheric Administration (NOAA), accessed through: <https://www.ngdc.noaa.gov/geomag/calculators/magcalc.shtml?useFullSite=true>

To support the research, all data were processed using several software programs that are compatible with spatial data processing. These include Qimera, a bathymetry data processing software; Fledermaus FMGT, a backscatter data

processing software; Oasis Montaj, a magnetic anomaly data processing software; and other general spatial data software.

2.3 Data Processing

The data processing phase for generating an analysis of the potential presence of hydrocarbons in the study area consists of several steps. Preparation for multibeam echosounder data processing includes patch test data calibration, raw data file preparation, tidal correction data, and sound velocity correction data. Patch test calibration using Qimera software is performed to correct the instrument's sensors in multibeam echosounder data processing. Patch test calibration includes roll, pitch, and yaw (heading). Raw multibeam echosounder data (*.all) is corrected using tidal data (*.tid) and sound velocity data (*.asvp). The corrected data is cleaned of noise and spikes. Data cleaning is performed using Qimera software and produces output in the form of depth data (*.asc) and other formats (*.gsf) used in backscatter processing.

The depth data (*.asc) is then layout-processed using spatial data processing software to produce a bathymetric map. Data in *.gsf format is used in Fledermaus FMGT software to perform mosaic and then perform ARA analysis, which will help in classifying the types of seabed sediment based on the characteristics of the acoustic signal reflection that occurs [8]. Magnetometer data processing is carried out with daily data correction (diurnal) and IGRF correction.

Daily data correction (diurnal) is carried out to reduce the impact of differences in acquisition time and solar radiation [9].

$$\Delta H = H_{total} \pm \Delta h_{daily} \tag{1}$$

information:

H_{total} : Total daily correction value
 Δh_{daily} : Difference in daily values

IGRF correction is carried out to reduce the influence of the Earth's main magnetic field on the acquisition data [9].

$$\Delta H = H_{total} \pm \Delta h_{daily} \pm H0 \tag{2}$$

information:

H_{total} : Total daily correction value
 Δh_{daily} : Difference in daily values
 $H0$: International Geomagnetic Reference Field (IGRF)

After that, the Gridding process is carried out to obtain an overview of the total magnetic field anomaly value. Reduction to the equator is carried out on the residual anomaly data to form a magnetic anomaly pattern into a monopole, thus simplifying the analysis process [10]. The separation of regional and residual magnetic field anomalies from the total magnetic field is carried out using a Butterworth filter. The separation produces regional anomaly data and residual anomaly data.

3 RESULT AND DISCUSSION

3.1 Depth Determination

The bathymetric data comes from the 2023 Jala Citra III Expedition. The area surveyed in May 2023 included 90 lanes within the Alor Basin. Data processing was performed using Qimera software. The process began with sensor corrections, including patch tests and data corrections, utilizing sound velocity and tidal data. This processing used a

resolution of $0.000898^\circ \times 0.000898^\circ$ due to the large processing area. Afterward, the data were cleaned to remove noise and spikes to produce a corrected bathymetric map.

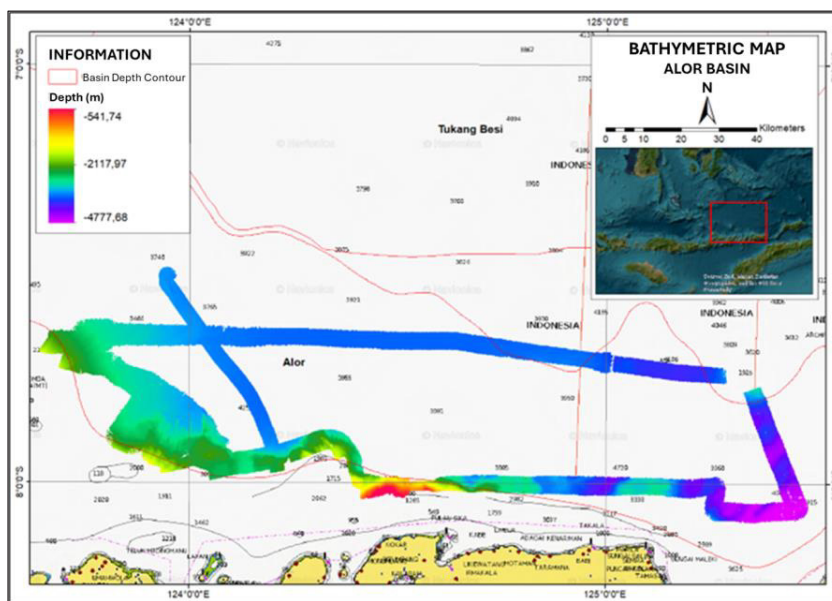


Fig. 2. Bathymetric Map of the Research Location

The processing yields varying depths and marine morphology visible from various angles. Overall, the data indicate that the waters in the Alor Basin are deep waters, namely bathyal and abyssal zones [11]. The average depth value of the measurement area is 3643 m, with the maximum depth value in the southeast showing a depth of up to 4777.68 m. On the east side, there is a steep slope due to the presence of seamounts outside the basin area, namely Baruna Komba and Abang Komba, and in the southern part of the basin is closer to the Flores Islands. Meanwhile, the central area to the eastern side shows a gentler depth but with deeper values.

3.2 Acoustic Backscatter Value

Backscatter data processing was performed using the corrected data. The data was processed using FMGT software. Processing began with configuration settings and the creation of mosaics containing intensity values. These intensity values will be used in Angular Response Analysis (ARA) to classify sediment types in the Alor Basin.



Fig. 3. Backscatter Mosaic Building Results

The mosaic creation results are shown in Figure 3. The resulting mosaics have a range of values indicating variations in backscatter intensity across the area. The study area has an intensity between -0.65 and -0.35 dB. Backscatter mosaics with high energy are indicated by light colors, while mosaics with dark colors indicate low energy.

ARA processing indicates that almost the entire study area has similar sediment types. The visualization in Figure 4 shows that clay sediment types dominate the study area. The Angular Response Curve was used to assess the level of uniformity of seabed material on the surface and identify the suitability of the mosaic data between the right and left sides of the nadir. The blue curve in Figure 6 shows a symmetrical trend in average reflectance with a peak around the nadir angle (90°) and decreases towards smaller angles. The red and green curves represent actual data from the left and right sides of the nadir. Fluctuations in both curves reflect variations in seabed surface reflectance classified as clay with patterns that experience slight deviations due to surface irregularities or local conditions. This is consistent with the Seabed Surface Sediment Map published by the Center for Marine Geology Research and Development (2010), which reveals mud sediment types, primarily silt and clay containing 20% sand, including blue mud, green mud and clay, black mud and clay, coral mud, volcanic glass, volcanic mud, gray clay, and sandy mud [12].



Fig. 4. The Result of *Angular Response Analysis*

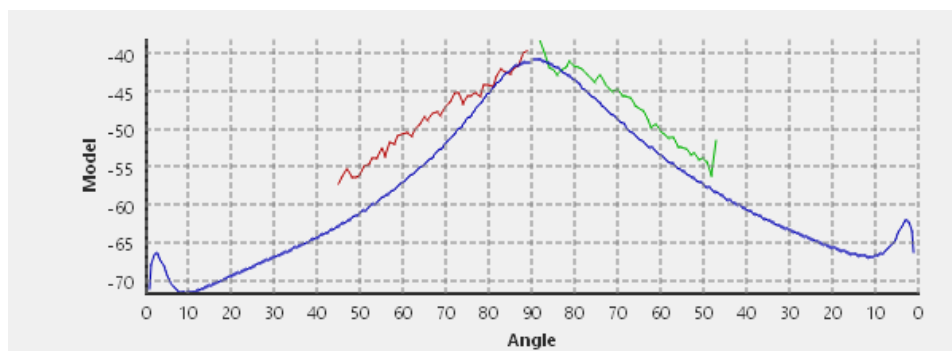


Fig. 5. *Angular Response Curve*

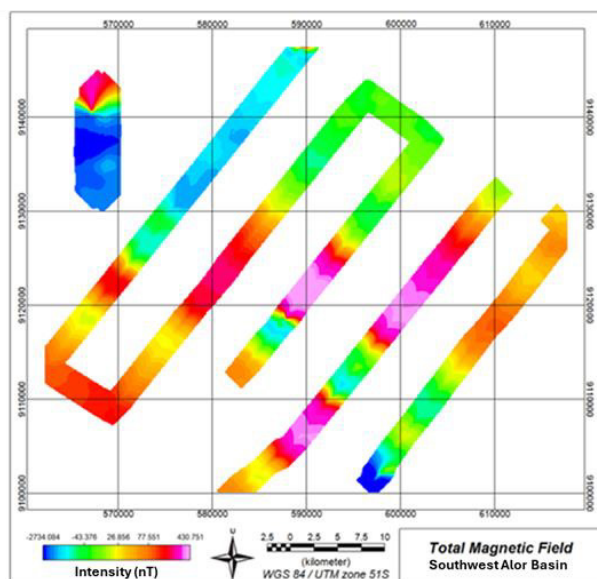
A variety of geological information can be obtained from sediment analysis, reflecting the geological processes and dynamics of a region. The Alor Basin is part of a deep marine basin characterized by low energy and slow sedimentation rates, which strongly support the deposition of fine particles such as clay. Clay can accumulate with other deep-sea materials such as radiolarians and foraminifera. Clay is thought to originate from volcanic ash transformed into clay minerals such as montmorillonite and illite, as well as from the weathering of rocks on land that are then carried to the sea by rivers or ocean currents. Furthermore, hydrothermal activity on the seafloor can also produce certain types of clay, such as smectite.

3.3 Magnetic Anomaly

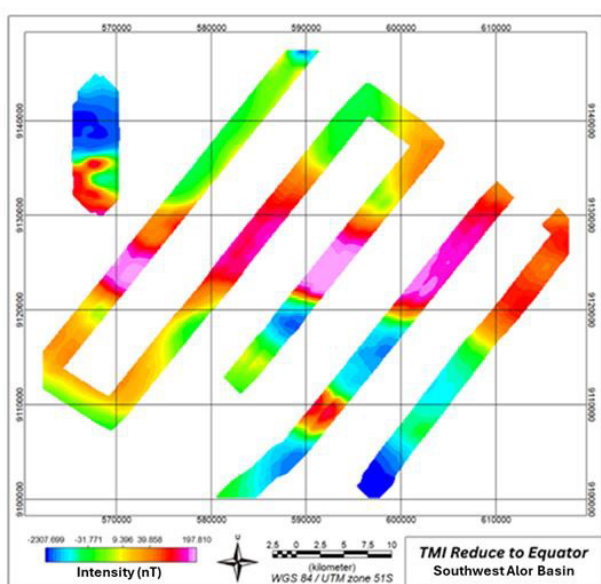
Magnetic data was processed using the Oasis Montaj software. These magnetic field variations are caused by the contrast or distribution of magnetic properties between rock types within the Earth's crust. This results in a non-uniform Earth's magnetic field, known as a magnetic anomaly. The total magnetic field intensity map was obtained after performing diurnal correction and IGRF correction. Figure 6(a) displays the total magnetic field intensity results. This map still has a dipole shape, requiring reduction toward the equator to make it a monopole for easier interpretation. Figure 6(b) shows the total magnetic field intensity results after being reduced toward the equator and

converted to a monopole. The resulting total magnetic anomaly values range from -2307.669 nT to 197.810 nT. However, this value is a combination of regional and residual magnetic values.

Separating regional and residual anomalies requires depth information from the measured data. Therefore, depth estimation was performed using the radially averaged power spectrum method. The regional zone has a depth of almost 4000 m, the residual zone is at a depth of around 1500 m, while white noise appears at a depth of around 1000 m. This corresponds to the seabed depth values obtained in the area. The regional zone is characterized by a sharply decreasing graph, while the residual zone shows a more gradual graph. The gradient shift indicating the boundary between the zones occurs on the x-axis at a value of 0.45 km^{-1} and 1.12 km^{-1} .



(a)



(b)

Fig. 6. Total Magnetic Intensity and Equatorial Reduced TMI

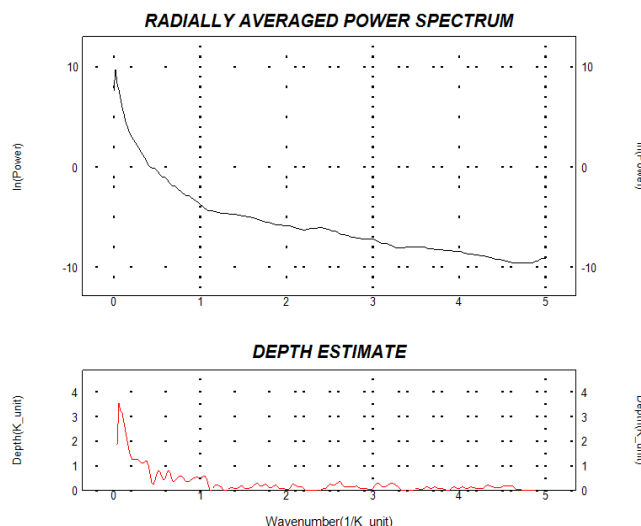


Fig. 7. The Graph of Radially Averaged Spectrum and Depth Estimate

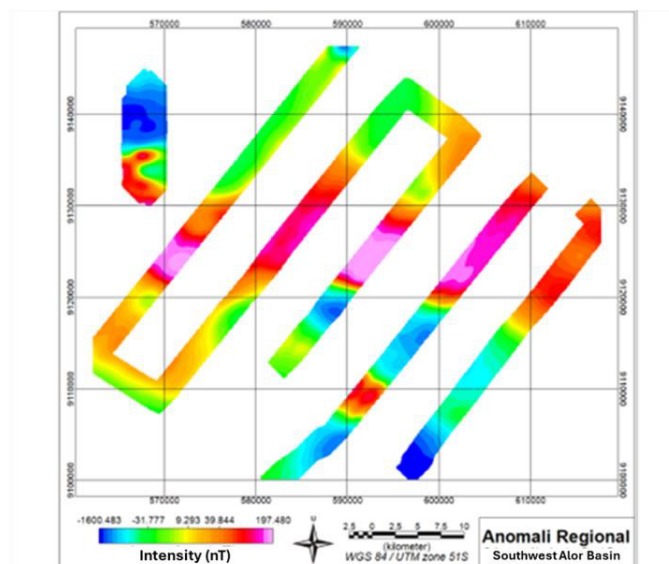


Fig. 8. Regional Anomaly Separation Results

Anomaly separation was performed using a Butterworth filter of degree 8. The choice of central wavelength depended on the resulting graph. For regional anomalies, a central wavelength of 1540 was used, and for residual anomalies, a central wavelength of 2860 was used. Figure 8 visually demonstrates the differences between regional and residual anomalies. Regional anomalies represent regional subsurface conditions, covering a large area and at significant depths, resulting in homogenous rock characteristics with minimal striking geological structural contrasts. In contrast to regional anomalies, residual anomalies provide geological information at shallower depths. This presents heterogeneity in the rock composition and the possibility of a more diverse range of geological structures.

The similar colors in Figures 8 and 9 for regional and residual anomalies do not necessarily reflect the same magnetic field values. The magnetic field values for regional anomalies range from -1600.483 nT to 197.480 nT. Meanwhile, the magnetic field values for residual anomalies range from -1031.022 nT to 361.214 nT. Both are nearly identical. Residuals have a smaller negative range and a larger positive range than regional anomalies. A magnetic field value that tends to be negative indicates the presence of lithology with a low level of magnetization. Another possibility is

that the area was previously composed of highly magnetized rocks, but underwent hydrothermal alteration or certain chemical reactions that caused demagnetization in the rocks. Conversely, a positive range of magnetic field values reflects the presence of ferromagnetic or highly magnetized materials and the possibility of an increase in magnetization in the host rock (country rock). Anomaly boundaries have been identified in the residuals, with positive anomalies indicating the presence of mining or mineral deposits, while negative anomalies indicate the presence of petroleum deposits [13].

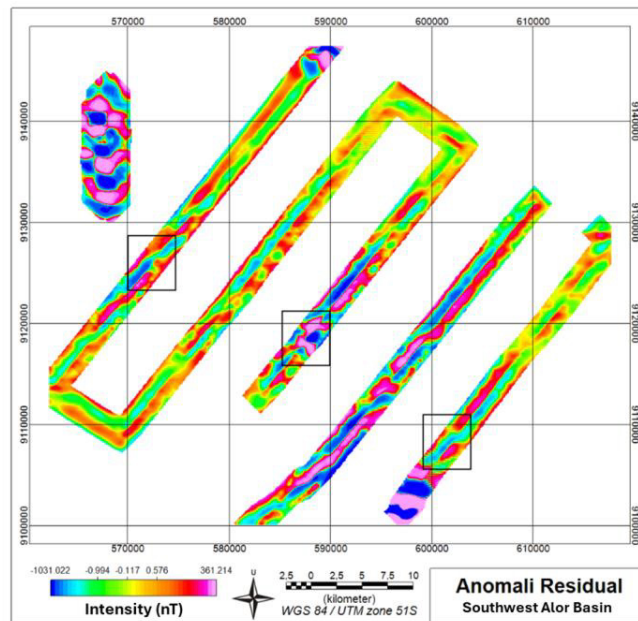


Fig. 9. Residual Anomaly Separation Results

Striking differences in values occur in several areas marked with color. Figure 9 shows significant magnetic activity in the three areas shown. The differences in magnetic values found indicate tectonic activity. This is in line with the discovery of faults in previous research [14]. The faults were identified as NW-SE oriented, which is in line with the formation of the seamounts in the area, namely Baruna Komba and Abang Komba.

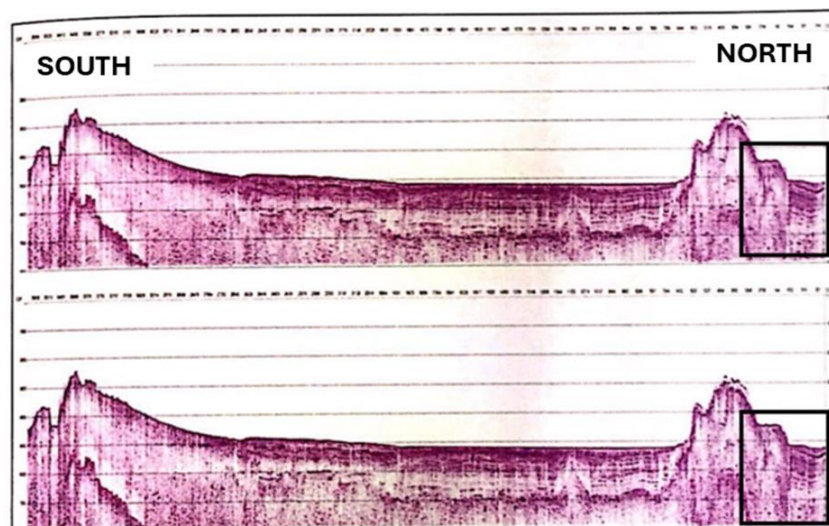


Fig. 10. Seismic Cross-Section Results of Track 6 Post-Stack Migration Results (Top) and Pre-Stack Migration Results (Bottom) [15]

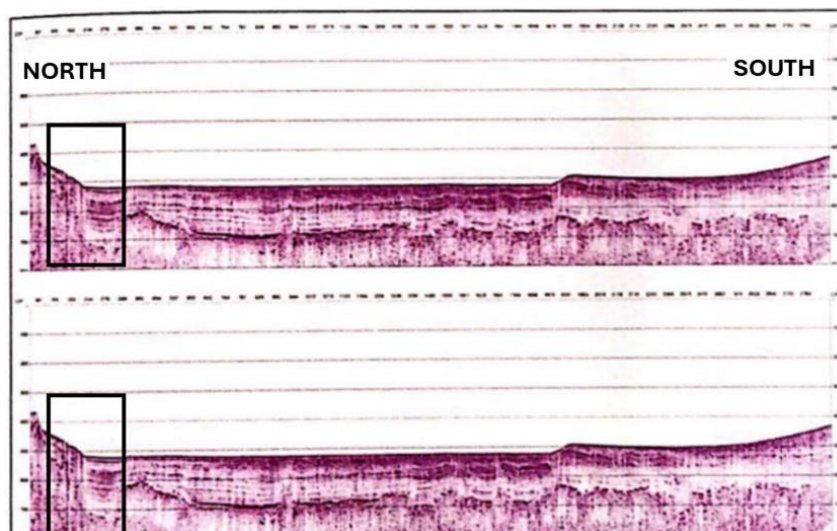


Fig. 11. Seismic Cross-Section Results of Track 8 Post-Stack Migration Results (Top) and Pre-Stack Migration Results (Bottom) [15]

3.4 Seismic Analysis

The seismic data used were processed by the Center for Marine Geology Research and Development (P3GL) in 2014 [15]. The data were collected in Alor waters at LP 2308 and LP 2309, which are located in the same location as this research area. Tracks 6 and 8 in the P3GL report are similar to the magnetometer data collection area. The seismic data oriented south-north and north-south, respectively, revealing rock layers. One of these layers exhibits a fault, supporting the analysis of the magnetic anomaly data. Figure 11 shows a steep morphology in the north and irregularities and shifts in the reflector layer on the right side of the cross-section, indicating the presence of a fault structure. This fault is characterized by a discontinuous layer and indicates vertical displacement. Meanwhile, Figure 12 shows a relatively flat seabed surface, but on the north side, there is a shift in the reflector layer, also indicating the presence of a fault. The presence of this fault can function as a migration route or even a structural trap for hydrocarbons. The relatively flat and consistent reflective layers in the center of the section likely represent reservoir rock layers, while the shift in the fault could create a closed zone that allows hydrocarbons to accumulate. Thus, the fault structure observed in this seismic section not only demonstrates the dynamics of the underwater geology but also serves as an important indicator in assessing the potential for hydrocarbon deposits in the area.

4 CONCLUSION

The Alor Basin has an identified depth of up to 4,777.68 m, with the topmost sedimentary layer being clay. The Alor Basin is part of a deep marine basin characterized by low energy and slow sedimentation rates, thus favoring the deposition of fine particles such as clay. Clay can accumulate with other deep-sea materials such as radiolarians and foraminifera. The presence of clay in the Alor Basin has the potential to support petroleum systems. Clay can act as a source rock if it contains organic matter or as a cap rock due to its impermeable nature. The differences in magnetic anomaly intensity recorded in the area are quite significant due to indications of tectonic activity. This is supported by research by P3GL in 2014 using seismic sections. The presence of these faults can function as migration pathways or even structural traps for hydrocarbons. Faults can act as migration pathways for hydrocarbons from source rock to reservoir rock. Furthermore, faults can also create complex geological conditions that support hydrocarbon accumulation, such as fault traps or fault-cut anticlines.

The results of this study still require further research. This study only indicates that magnetic anomalies exist beneath the seabed of the Alor Basin due to tectonic activity. Integration of other geophysical data, such as regional geology and the structure of the rocks forming it, as well as surface and subsurface geological analysis, is needed to confirm the existence of structures that could potentially act as hydrocarbon traps.

ACKNOWLEDGEMENT

The author would like to thank all parties who assisted and supported the Geomarine Laboratory lecturers who assisted in conducting this research. He also thanks the Indonesian Navy's Hydrological Research Center (Pushidros TNI AL) and the Indonesian National Marine Research and Development Agency (BBSPGL) for providing limited data to assist in this research. The authors also gratefully acknowledge financial support from the Institut Teknologi Sepuluh Nopember for this work, under the project scheme of the Publication Writing and IPR Incentive Program (PPHKI) 2025.

REFERENCE

- [1] A. Cahyono, "Masifkan Eksplorasi, 68 Cekungan Migas Simpan Potensi Besar," Kementerian Energi dan Sumber Daya Mineral. Diakses: 5 Januari 2025. [Daring]. Tersedia pada: <https://www.esdm.go.id/id/media-center/arsip-berita/masifkan-eksplorasi-68-cekungan-migas-simpan-potensi-besar>
- [2] G. A. S. Nayoan, "Offshore Hydrocarbon Potential of Indonesia," *Energy*, vol. 11, no. 6, hlm. 1225–1246, 1981, doi: 10.1016/0360-5442(81)90034-7.
- [3] R. W. V Bemmelen, *The Geology of Indonesia: General Geology of Indonesia and Adjacent Archipelagoes*, vol. IA. The Hague: Government Printing Office, 1949.
- [4] P. G. McLeroy dan J. P. Riva, "Origin of Hydrocarbons," *Britannica*. Diakses: 5 Januari 2025. [Daring]. Tersedia pada: <https://www.britannica.com/science/petroleum/Origin-of-hydrocarbons>
- [5] Wahyudi, "Aplikasi Mikroseismik untuk Memindai dan Mengidentifikasi Keberadaan Hidrokarbon (Microseismic Application for Direct Hydrocarbon Detection and Identification)," *Berkala MIPA*, vol. 18, no. 2, hlm. 114–123, 2008, Diakses: 5 Januari 2025. [Daring]. Tersedia pada: <https://jurnal.ugm.ac.id/bimipa/article/view/33495>
- [6] K. Akbar, D. G. Pratomo, dan Khomsin, "Analisis Nilai Hambur Balik Sedimen Permukaan Dasar Perairan Menggunakan Data Multibeam Echosounder EM302," *Jurnal Teknik ITS*, vol. 6, no. 2, hlm. 2337–3520, 2017.
- [7] Moh. Ryan, J. R. Husain, dan H. Bakri, "Studi Anomali Magnetik Total untuk Pencarian Daerah Prospek Hidrokarbon Daerah Pulau Buru Provinsi Maluku," *Journal Geomine*, hlm. 17–21, 2015, doi: <https://dx.doi.org/10.33536/jg.v1i1.5>.
- [8] R. C. Hasan, D. Lerodionou, L. Laurenson, dan A. Schimel, "Integrating Multibeam Backscatter Angular Response, Mosaic and Bathymetry Data for Benthic Habitat Mapping," *PLoS One*, vol. 9, no. 5, Mei 2014, doi: 10.1371/journal.pone.0097339.
- [9] Ab. T. Insani, *Aplikasi Side Scan Sonar dan Magnetometer untuk Pemetaan Sebaran Anomali Magnetik Dasar Laut*. Malang: Institut Teknologi Nasional Malang, 2015.
- [10] A. H. Pinandita dan W. Sutresno, "Karakteristik Anomali Magnetik dari Metode Reduksi ke Kutub dan Reduksi ke Ekuator pada Struktur Sesar," *Globe: Publikasi Ilmu Teknik, Teknologi Kebumihan, Ilmu Perkapalan*, vol. 2, no. 3, hlm. 250–257, 2024, doi: 10.61132/globe.v2i3.515.
- [11] S. Puryono, S. Anggoro, Suryanti, dan I. S. Anwar, *Pengelolaan Pesisir dan laut Berbasis Ekosistem*. Badan Penerbit Universitas Diponegoro Semarang, 2019.
- [12] A. H. Satyana, "Geologi Kelautan Indonesia," 2022.
- [13] Diva Prameswari, *Analisis Pemodelan Inversi Data Geomagnet untuk Pemetaan Bawah Permukaan Cekungan Bone Sulawesi*. 2024.
- [14] L. Sarmili dan R. Arief Troa, "Keberadaan Sesar dan Hubungannya dengan Pembentukan Gunung Bawah Laut di Busur Belakang Perairan Komba, Nusa Tenggara," *Jurnal Geologi Kelautan*, vol. 12, no. 1, 2014.
- [15] Subarsyah, *Laporan Pengolahan Data Seismik 2D Multichannel Perairan Alor LP 2308 dan 2309*. 2014.